Published in final edited form as:
J Orthop Res. 2013 March ; 31(3): 343–349. doi:10.1002/jor.22236.

Dystrophin and Utrophin "Double Knockout" Dystrophic Mice Exhibit a Spectrum of Degenerative Musculoskeletal Abnormalities

Christian Isaac[1,2], **Adam Wright**[1,2], **Arvydas Usas**[1], **Hongshuai Li**[1], **Ying Tang**[1], **Xiaodong Mu**[1], **Nicholas Greco**[1,2], **Qing Dong**[2], **Nam Vo**[2], **James Kang**[2], **Bing Wang**[1,2], and **Johnny Huard**[1,2]

[1]Stem Cell Research Center, Bridgeside Point II, 450 Technology Dr, Suite 206, Pittsburgh, Pennsylvania 15219

[2]Department of Orthopaedic Surgery, University of Pittsburgh School of Medicine, Pittsburgh, Pennsylvania 15261

Abstract

Duchenne muscular dystrophy (DMD) is a degenerative muscle disorder characterized by the lack of dystrophin expression at the sarcolemma of muscle fibers. In addition, DMD patients acquire osteopenia, fragility fractures, and scoliosis indicating that a deficiency in skeletal homeostasis coexists but little is known about the effects of DMD on bone and other connective tissues within the musculoskeletal system. Recent evidence has emerged implicating adult stem cell dysfunction in DMD myopathogenesis. Given the common mesenchymal origin of muscle and bone, we sought to investigate bone and other musculoskeletal tissues in a DMD mouse model. Here, we report that *dystrophin–utrophin* double knockout (*dko*) mice exhibit a spectrum of degenerative changes, outside skeletal muscle, in bone, articular cartilage, and intervertebral discs, in addition to reduced lifespan, muscle degeneration, spinal deformity, and cardiomyopathy previously reported. We also report these mice to have a reduced capacity for bone healing and exhibit spontaneous heterotopic ossification in the hind limb muscles. Therefore, we propose the *dko* mouse as a model for premature musculoskeletal aging and posit that a similar phenomenon may occur in patients with DMD.

Keywords

muscular dystrophy; osteopenia; bone healing; ectopic calcification; proteoglycans

Duchenne muscular dystrophy (DMD) is an X-linked, recessive, degenerative muscle disease that is characterized by the wasting of skeletal muscle, progressive muscular weakness, and premature death, usually from cardiorespiratory failure.[1,2] A congenital mutation on chromosome Xp21.2, which results in the absence of functional dystrophin in skeletal muscle and neuronal tissues, can occur up to three times in every 10,000 live male

Correspondence to: Johnny Huard (T: 412-648-2798; F: 412-648-4066; jhuard@pitt.edu).

births and is the genetic event that initiates the pathogenesis of the disease.[2–4] The lack of dystrophin expression compromises the integrity of the sarcolemma, rendering myofibers abnormally fragile, but despite the absence of dystrophin at birth, boys who harbor DMD mutations appear relatively normal until the age of four or five.[2,5] Unfortunately, skeletal muscle degeneration occurs rapidly thereafter, with wheelchair and ventilator dependence occurring at the beginning and end of the second decade, respectively. Currently, only palliative treatments are available.[2]

Myofiber regeneration in DMD is thought to be mediated by adult stem/progenitor cells and/or satellite cells.[6] Dystrophin mutations are not expressed in muscle satellite cells but repetitive cycles of degeneration and regeneration ensue because the newly differentiated myofibers lack functional dystrophin.[7–12] As a result, there is a decline in the replicative ability of muscle progenitor cells and a progressive decrease in regenerative capacity.[13] Therefore, adult stem cell exhaustion has been implicated in the clinical manifestation of DMD and is thought to play a key role in disease progression.

Despite the tissue-limited expression of dystrophin, the pathology associated with DMD is not limited to skeletal and cardiac muscle. Children with DMD may acquire a host of debilitating skeletal problems including osteopenia, fragility fractures, and scoliosis.[1,14–18] For the most part, osteopenia has been blamed on skeletal muscle degeneration because attenuated muscular forces and a lack of bone mechanical stimuli can be detrimental to bone mineral density.[19–22] As a result, few studies have investigated the perturbation of the disease on tissues outside of skeletal muscle, and thus, little is known about the precise effects of DMD on bone and other musculoskeletal tissues.[23–27]

In this study, we sought to investigate the effects of DMD on the musculoskeletal system using a DMD mouse model. The *mdx* (X-chromosome-linked muscular dystrophy) and *dko* (*dystrophin–utrophin* double knockout) mice represent two such models. The *mdx* mouse lacks functional dystrophin but the DMD phenotype is relatively mild compared to the human disease.[28–33] Since utrophin, a dystrophin-related protein, is able to compensate for the loss of dystrophin, both utrophin and dystrophin loss results in a more severe phenotype than the *mdx* mouse.[34,35] Here, we report a spectrum of degenerative changes, outside of skeletal muscle, in bone, articular cartilage, and intervertebral discs of *dko* mice. In addition, we find these mice to exhibit delayed bone healing, and at a young age, *dko* mice accumulate diffuse soft-tissue calcifications.

MATERIALS

Animals

C57BL/10 mice were obtained from Jackson Laboratories (Bar Harbor, ME). The *mdx* and *dko* mice were derived from our colony and housed in groups of four on a 12:12 h light–dark cycle at 20–23°C. All procedures were approved by the Institutional Animal Care and Use Committee at the University of Pittsburgh (IACUC protocol number 0804625B-4).

Micro-Computed Tomography

At 6 weeks old, mice were anesthetized with isoflurane and supplemental O_2 gas, and the lower extremities, including the pelvis, was scanned using the Viva CT 40 (Scanco, Switzerland) with settings: energy 70 kvP, intensity 114 μA, integration time 200 ms, isotropic voxel size 35 μm, threshold 163.

Bone Healing

At 5 weeks old, mice were sedated as above, and an antero-medial incision was made over the right knee and the proximal tibia exposed. A unicortical, spherical defect was created using a 0.9 mm burr (Fine Science Tools). The wound was irrigated and closed with 4-0 prolene. Mice were injected post-operatively with subcutaneous buprenorphine at 0.1 mg/kg. Bone in-growth was evaluated with serial micro-CT on postoperative days 1, 7, and 14. Total defect area was calculated by measuring the length of the defect on each axial slice.

Tissue Histology

Mice were sacrificed in CO_2 chamber according to the IACUC protocol. Bone tissue was dissected using sterile techniques and fixed in formalin for 24 h before being sectioned in freezing media. For von Kossa staining, sections were hydrated and incubated with 1% silver nitrate under ultraviolet light for 20 min, 5% sodium thiosulfate for 5 min, and mounted. For Masson trichrome staining, sections were incubated in Weigert's iron hematoxylin working solution for 10 min, rinsed, transferred to Biebrich scarlet-acid fuchsin solution for 15 min before direct incubation in aniline blue solution for 5 min. For safranin O staining, sections were stained in Weigert's iron hematoxylin working solution for 4 min, destained in fresh acid alcohol for 1 min, rinsed, incubated in 0.02% aqueous fast green for 5 min, washed in 1% acetic acid for 30 s, stained in 0.1% aqueous safranin O for 5–7 min, and mounted in synthetic resin. Gluteus maximus tissue was frozen in liquid nitrogen using freezing medium, sectioned, and slides were incubated for 5 min in alizarin red solution, counterstained with eosin. All slides were analyzed using a light microscope (Nikon Eclipse E800, Tokyo, Japan). Images were obtained under 4–20× magnification (Q-imaging RETIGA, Surrey, British Columbia, Canada). Isolated spines were decalcified and embedded in paraffin (Tissue Tek processor and Leica embedder). 7 μm sections were stained with safranin O and fast green dyes (Fisher Scientific, Pittsburgh, PA) and photographed at 4–20× magnification (Nikon Eclipse Ts100).

Statistical Analyses

All experiments were performed using at least three different animals in each group, and mean, standard deviation, and sample size were used to calculate statistical significances using Student's *t*-test.

RESULTS

Bone Abnormalities in *dko*$^{-/-}$ Mice

In order to evaluate the bone morphometry in *dko* mice, the proximal tibia, in 6-week-old male, wild-type, *mdx*, *dko* heterozygous (*dko*$^{+/-}$ or *mdx; utrn*$^{+/-}$), and *dko* homozygous

(*dko*$^{-/-}$ or *mdx; utrn*$^{-/-}$) mice, was analyzed using micro-computed tomography (micro-CT). The metaphyseal–diaphyseal cortex of the proximal tibia in *dko*$^{-/-}$ mice was consistently thinner and there were less metaphyseal trabeculae (Fig. 1A). Next, we used the CT's evaluation software to determine proximal tibia bone volume and density. We observed a significant reduction in the average bone volume and density of *dko*$^{-/-}$ mice when compared to controls (Fig. 1B, C). We then performed trabecular bone analysis in order to determine the relative thickness of trabeculae in the proximal tibia of *dko*$^{-/-}$ mice. Compared to control animals, we found the thickness of *dko*$^{-/-}$ trabeculae to be significantly lower (Fig. 1D).

In order to further investigate the differences in bone morphometry determined by micro-CT evaluation, we processed the proximal tibias of *dko*$^{-/-}$ mice for histological analysis using von Kossa (bone mineralization) and Masson trichrome blue staining (collagen content). Age-matched *wild-type*, *mdx*, and *dko*$^{+/-}$ tibias were included as controls. Consistent with our micro-CT data, we observed fewer, and thinner, trabeculae in the *dko*$^{-/-}$ proximal tibia when compared to the controls (Fig. 2A). Similar results were obtained when trichrome staining was employed. Next, we determined the relative amount of collagen in the metaphyseal bone from *dko*$^{-/-}$ animals by quantifying the trichrome positive areas (Fig. 2B). We observed a significant decrease in the amount of collagen detectable in *dko*$^{+/-}$ and *dko*$^{-/-}$ bone when compared to *wild-type* and *mdx* bone; however, this collagen discrepancy was most severe in the metaphyseal bone obtained from the *dko*$^{-/-}$ mice.

Delayed Bone Healing in *dko*$^{-/-}$ Mice

In order to investigate the mechanisms contributing to abnormal bone formation in *dko*$^{-/-}$ mice we tested osteogenesis in vivo using a bone defect model. Five-week-old *dko*$^{-/-}$ mice were age-matched with control animals and a spherical, unicortical defect was surgically created in the proximal tibia. The mice were followed with serial micro-CT scans to monitor bony ingrowth at 1 and 2 weeks post-operation. The area of defect coverage was determined in comparison to the defect coverage within 24 h (Fig. 3A). The *dko*$^{-/-}$ mice had significantly less bony in-growth at weeks 1 and 2 compared to the *mdx* and wild-type control animals, respectively (Fig. 3B). Intriguingly, during these experiments, the *mdx* mice made new bone faster than wild-type controls, showing significantly more bony ingrowth at 1 week. After 2 weeks, however, there was no detectable difference between these two groups.

Ectopic Calcification in Muscle of *dko*$^{-/-}$ Mice

During the micro-CT evaluations of *dko*$^{-/-}$ mice, we repeatedly observed diffuse, scattered, radio-opaque collections within the muscle tissue of the bilateral hind limbs (Fig. 4A, B, arrows). In order to further investigate these collections we analyzed 6-week-old *dko*$^{-/-}$ mice by micro-CT. Age-matched wild-type, *mdx*, and *dko*$^{+/-}$ animals were included as controls. We observed the presence of ectopic calcification in two-thirds of the *dko*$^{-/-}$ mice ($n = 6$). In comparison, similar collections were not found in any control mice ($n = 6$ from each control group). In order to confirm the nature of these collections we harvested gluteus maximus muscles from 6-week-old *dko*$^{-/-}$ mice and included age-matched wild-type muscle as controls. These tissues were processed for histological analysis using alizarin red staining for calcium. Muscle obtained from *dko*$^{-/-}$ mice showed positive alizarin red staining

whereas there was no detectable calcium in control muscle (Fig. 4C). Therefore, the radio-opaque collections seen on micro-CT are deposits of ectopic calcification.

Degenerative Changes in Articular Cartilage and Intervertebral Discs of *dko*$^{-/-}$ Mice

The loss of proteoglycans (PGs) from articular cartilage and intervertebral discs is indicative of degenerative changes and is a hallmark of human degenerative joint disease (DJD) and degenerative disc disease (DDD).[36,37] Therefore, we performed a histological analysis of the proximal tibia and spinal intervertebral discs isolated from male *dko*$^{-/-}$ mice and evaluated the PG content using safranin O and fast green stains. Figure 5A shows a representative image of 7-week-old *dko*$^{-/-}$ proximal tibia articular and growth plate cartilage and illustrates the loss of PGs, in contrast to control *mdx* and *wild-type* tibias. Interestingly, the tibial growth plate displayed a similar loss of PGs toward the proximal aspect. Likewise, Figure 5B shows a representative image of a 4-week-old *dko*$^{-/-}$ intervertebral disc and illustrates a relative loss of PGs and disorganization within the disc, most pronounced at the nucleus pulposus, when compared to *mdx* and *wild-type* controls.

DISCUSSION

Our micro CT and histological analyses of the proximal tibia in the *dko*$^{-/-}$ mice indicated a deficiency in cortical and trabecular bone, marked by a significant decrease in bone volume and density, which correlated with a loss of bone collagen content. Few studies have looked at musculoskeletal effects outside of the myopathic changes in humans; however, those studies have discovered alterations in bone micro-architecture and bone metabolism that coincide with our findings in the *dko* model. One of the earlier investigations found that patients diagnosed with DMD have decreased bone density, increased bone turnover, and low 25-OH Vitamin D.[38] Importantly, this was demonstrated in DMD patients with and without gluccocorticoid therapy, since gluccocorticoid acts as a confounder with its beneficial effect on decreasing muscle inflammation but concurrent suppression of bone formation. Further research has focused on DMD patients taking gluccocorticoids because of the increasing prevalence of treatment and it has continued to be shown that these patients have significantly lower bone mineral density and bone mineral content compared to healthy controls.[39] These results are consistent with the clinically observed osteopenia in DMD patients and research performed by Novotny et al.[26] using a murine model, which indicates that a deficiency in extracellular matrix (ECM) production may contribute to abnormal bone formation in the *dko*$^{-/-}$ mice. This may be a direct or indirect consequence of the lack of dystrophin expression, given the role of dystrophin and utrophin in linking the actin cytoskeleton to the ECM and the known effect of sarcopenia on bone;[2,40–42] however, a delay in bone healing, as observed in this study, suggests a deficiency in osteoblast activity may exist in *dko*$^{-/-}$ mice. It is interesting that age-matched *mdx* mice show a robust bone healing response compared to the wild-type controls. At this age, *mdx* mice are known to mount a large regenerative effort in response to muscle degeneration and perhaps this process may influence bone healing.[33] Regardless, it will be important in the future to explore the osteogenic capacity of adult stem cells obtained from *mdx* and *dko* mice given the implication of stem cell exhaustion in the pathogenesis of DMD combined with the results of this study.

DJD of the knee and DDD of the spine can occur with normal aging in humans.[43,44] It is unclear if patients with DMD are prone to the early development of either wear-related, degenerative musculoskeletal conditions because most patients will not live long into their third decade and confounding issues exist that could prevent the identification of such problems. For example, symptomatic pain from osteoarthritis typically occurs after weight-bearing activity, and unfortunately, patients with DMD are unable to perform such activities due to their illness.[45] As a result, there is rarely a time after wheelchair dependence that a weight bearing joint will be exposed to a significant mechanical load. In addition, joint range of motion becomes significantly impaired by the acquisition of joint contractures.[46] Similarly, DDD typically causes neurogenic lower back pain, but in the presence of scoliosis it may not be clinically obvious.[47] The etiology of articular cartilage and disc degeneration in *dko*$^{-/-}$ mice is unclear at this time; however, it is interesting that the cartilaginous growth plate also lacks PGs because this suggests a problem with chondrogenesis, and thus stem/progenitor cell function, rather than excessive, premature biomechanical wear.

Literature concerning other DMD animal models is scarce. One such murine model consisting of a dy/dy genotype exhibits a severe dystrophic phenotype. Studies have demonstrated the adverse osseous effects that are present in this dystrophic model. These mice have significantly stunted growth of their long bones in the radius, ulna, humerus, femur, and tibia, which was shown by comparing the bone lengths to healthy controls.[48] A more recent study by Garris et al.[49] confirmed the bone length of the femur and tibia as well as the pelvis to be significantly shorter in the dy/dy mice. They have further shown that at the cellular level the osteocyte density in the tibia is significantly decreased. Therefore, it is possible that the bone alterations may be related to the severe muscular dystrophic phenotype in these various models, but it is still evident from this research that the *dko* model displays similar phenotypic changes as compared to human DMD subjects making it a valuable model for studying the biological manifestations of DMD.

Skeletal muscle degeneration, cardiomyopathy, and spinal deformity are known to occur in DMD patients and *dko*$^{-/-}$ mice. In this study, we showed that *dko*$^{-/-}$ mice also develop degenerative changes to bone, cartilage, and intervertebral discs. Such degenerative conditions may occur in normal aging. Furthermore, problems with tissue healing and ectopic calcification are also associated with aging. Thus, the problems with bone healing and ectopic calcification characterized by this study support a phenomenon of accelerated musculoskeletal aging in *dko*$^{-/-}$ mice. Aging of the human population predicts an increased incidence of age-related, degenerative musculoskeletal conditions, not limited to osteoporosis, fragility fractures, DJD, and DDD.[50–52] A mouse model of musculoskeletal degeneration, such as the *dko* model, can provide a research tool to further our understanding of conditions associated with aging. In terms of DMD, given the spectrum of the pathology in the mesenchymal tissues, and emerging evidence that implicates the exhaustion of myogenic stem/progenitor cells in DMD pathogenesis, one must consider a problem exists, either primarily or secondarily, in the adult stem cell compartment. Adult stem cells and muscle-derived stem/progenitor cells are tightly associated with aging.[53,54] If the congenital absence of dystrophin from skeletal muscle and neuronal tissues eventually leads to myogenic stem cell exhaustion with implications toward homeostasis of other

mesenchymal tissues via stem cell depletion, then gene therapy to replace dystrophin loss will predictably falter unless instituted very early or at least before significant attrition in stem cell numbers occur. This may prove technically challenging given the diagnosis of DMD is typically delayed until age 4. Furthermore, if future medical advances are able to rescue the skeletal muscle phenotype in DMD patients, then these patients may be at risk for acquiring other degenerative musculoskeletal diseases, such as DJD and DDD. Thus, further studies are critical for us to understand these biological processes and to develop effective therapies for the treatment of DMD. This work not only warrants an investigation into adult stem cell characterization in *dko* mice, but also highlights the essentials of understanding the role of stem cell function in DMD and common musculoskeletal conditions associated with aging.

Acknowledgments

This work was supported in part by the Henry J. Mankin endowed chair at the University of Pittsburgh, the William F. and Jean W. Donaldson endowed chair at the Children's Hospital of Pittsburgh and the Department of Defense (W81XWH-09-1-0658).

References

1. Larson CM, Henderson RC. Bone mineral density and fractures in boys with Duchenne muscular dystrophy. J Pediatr Orthop. 2000; 20:71–74. [PubMed: 10641693]
2. Sussman M. Duchenne muscular dystrophy. J Am Acad Orthop Surg. 2002; 10:138–151. [PubMed: 11929208]
3. Koenig M, Hoffman EP, Bertelson CJ, et al. Complete cloning of the Duchenne muscular dystrophy (DMD) cDNA and preliminary genomic organization of the DMD gene in normal and affected individuals. Cell. 1987; 50:509–517. [PubMed: 3607877]
4. Hoffman EP, Fischbeck KH, Brown RH, et al. Characterization of dystrophin in muscle-biopsy specimens from patients with Duchenne's or Becker's muscular dystrophy. N Engl J Med. 1988; 318:1363–1368. [PubMed: 3285207]
5. Infante JP, Huszagh VA. Mechanisms of resistance to pathogenesis in muscular dystrophies. Mol Cell Biochem. 1999; 195:155–167. [PubMed: 10395079]
6. Sacco A, Mourkioti F, Tran R, et al. Short telomeres and stem cell exhaustion model Duchenne muscular dystrophy in mdx/mTR mice. Cell. 2010; 143:1059–1071. [PubMed: 21145579]
7. Morgan JE, Zammit PS. Direct effects of the pathogenic mutation on satellite cell function in muscular dystrophy. Exp Cell Res. 2010; 316:3100–3108. [PubMed: 20546725]
8. Cornelison DD, Wilcox-Adelman SA, Goetinck PF, et al. Essential and separable roles for Syndecan-3 and Syndecan-4 in skeletal muscle development and regeneration. Genes Dev. 2004; 18:2231–2236. [PubMed: 15371336]
9. Collins CA, Olsen I, Zammit PS, et al. Stem cell function, self-renewal, and behavioral heterogeneity of cells from the adult muscle satellite cell niche. Cell. 2005; 122:289–301. [PubMed: 16051152]
10. Montarras D, Morgan J, Collins C, et al. Direct isolation of satellite cells for skeletal muscle regeneration. Science. 2005; 309:2064–2067. [PubMed: 16141372]
11. Kuang S, Kuroda K, Le Grand F, et al. Asymmetric self-renewal and commitment of satellite stem cells in muscle. Cell. 2007; 129:999–1010. [PubMed: 17540178]
12. Sacco A, Doyonnas R, Kraft P, et al. Self-renewal and expansion of single transplanted muscle stem cells. Nature. 2008; 456:502–506. [PubMed: 18806774]
13. Webster C, Blau HM. Accelerated age-related decline in replicative life-span of Duchenne muscular dystrophy myoblasts: implications for cell and gene therapy. Somat Cell Mol Genet. 1990; 16:557–565. [PubMed: 2267630]

14. Hsu JD. Skeletal changes in children with neuromuscular disorders. Prog Clin Biol Res. 1982; 101:553–557. [PubMed: 7156158]
15. McDonald DG, Kinali M, Gallagher AC, et al. Fracture prevalence in Duchenne muscular dystrophy. Dev Med Child Neurol. 2002; 44:695–698. [PubMed: 12418795]
16. Bothwell JE, Gordon KE, Dooley JM, et al. Vertebral fractures in boys with Duchenne muscular dystrophy. Clin Pediatr. 2003; 42:353–356.
17. Soderpalm AC, Magnusson P, Ahlander AC, et al. Bone markers and bone mineral density in Duchenne muscular dystrophy. J Musculoskel Neuron Interact. 2008; 8:24.
18. Karol LA. Scoliosis in patients with Duchenne muscular dystrophy. J Bone Joint Surg Am. 2007; 89:155–162. [PubMed: 17272432]
19. Boot AM, de Ridder MA, Pols HA, et al. Bone mineral density in children and adolescents: relation to puberty, calcium intake, and physical activity. J Clin Endocrinol Metab. 1997; 82:57–62. [PubMed: 8989233]
20. Ward K, Alsop C, Caulton J, et al. Low magnitude mechanical loading is osteogenic in children with disabling conditions. J Bone Miner Res. 2004; 19:360–369. [PubMed: 15040823]
21. Wang Q, Alen M, Nicholson P, et al. Weight-bearing, muscle loading and bone mineral accrual in pubertal girls—A 2-year longitudinal study. Bone. 2007; 40:1196–1202. [PubMed: 17258519]
22. McKay H, Smith E. Winning the battle against childhood physical inactivity: the key to bone strength? J Bone Miner Res. 2008; 23:980–985. [PubMed: 18318645]
23. Anderson JE, Lentz DL, Johnson RB. Recovery from disuse osteopenia coincident to restoration of muscle strength in mdx mice. Bone. 1993; 14:625–634. [PubMed: 8274305]
24. Montgomery E, Pennington C, Isales CM, et al. Muscle-bone interactions in dystrophin-deficient and myostatin-deficient mice. Anat Rec A Discov Mol Cell Evol Biol. 2005; 286:814–822. [PubMed: 16078270]
25. Nakagaki WR, Bertran CA, Matsumura CY, et al. Mechanical, biochemical and morphometric alterations in the femur of mdx mice. Bone. 2011; 48:372–379. [PubMed: 20850579]
26. Novotny SA, Warren GL, Lin AS, et al. Bone is functionally impaired in dystrophic mice but less so than skeletal muscle. Neuromuscul Disord. 2011; 21:183–193. [PubMed: 21256750]
27. Rufo A, Del Fattore A, Capulli M, et al. Mechanisms inducing low bone density in Duchenne muscular dystrophy in mice and humans. J Bone Miner Res. 2011; 26:1891–1903. [PubMed: 21509823]
28. Bulfield G, Siller WG, Wight PA, et al. X chromosome-linked muscular dystrophy (mdx) in the mouse. Proc Natl Acad Sci USA. 1984; 81:1189–1192. [PubMed: 6583703]
29. Sicinski P, Geng Y, Ryder-Cook AS, et al. The molecular basis of muscular dystrophy in the mdx mouse: a point mutation. Science. 1989; 244:1578–1580. [PubMed: 2662404]
30. Carnwath JW, Shotton DM. Muscular dystrophy in the mdx mouse: histopathology of the soleus and extensor digitorum longus muscles. J Neurol Sci. 1987; 80:39–54. [PubMed: 3612180]
31. Torres LF, Duchen LW. The mutant mdx: inherited myopathy in the mouse. Morphological studies of nerves, muscles and end-plates. Brain J Neurol. 1987; 110:269–299.
32. Coulton GR, Morgan JE, Partridge TA, et al. The mdx mouse skeletal muscle myopathy: I. A histological, morphometric and biochemical investigation. Neuropathol Appl Neurobiol. 1988; 14:53–70. [PubMed: 2967442]
33. DiMario JX, Uzman A, Strohman RC. Fiber regeneration is not persistent in dystrophic (MDX) mouse skeletal muscle. Dev Biol. 1991; 148:314–321. [PubMed: 1936568]
34. Deconinck AE, Rafael JA, Skinner JA, et al. Utrophin–dystrophin-deficient mice as a model for Duchenne muscular dystrophy. Cell. 1997; 90:717–727. [PubMed: 9288751]
35. Grady RM, Teng H, Nichol MC, et al. Skeletal and cardiac myopathies in mice lacking utrophin and dystrophin: a model for Duchenne muscular dystrophy. Cell. 1997; 90:729–738. [PubMed: 9288752]
36. Mankin HJ. Biochemical and metabolic aspects of osteoarthritis. Orthop Clin North Am. 1971; 2:19–31. [PubMed: 4940528]
37. Lyons G, Eisenstein SM, Sweet MB. Biochemical changes in intervertebral disc degeneration. Biochim Biophys Acta. 1981; 673:443–453. [PubMed: 7225426]

38. Bianchi ML, Mazzanti A, Galbiati E, et al. Bone mineral density and bone metabolism in Duchenne muscular dystrophy. Osteoporos Int. 2003; 14:761–767. [PubMed: 12897980]
39. Soderpalm AC, Magnusson P, Ahlander AC, et al. Low bone mineral density and decreased bone turnover in Duchenne muscular dystrophy. Neuromuscul Disord. 2007; 17:919–928. [PubMed: 17627820]
40. Winder SJ. The membrane-cytoskeleton interface: the role of dystrophin and utrophin. J Muscle Res Cell Motil. 1997; 18:617–629. [PubMed: 9429156]
41. Kamel HK. Sarcopenia and aging. Nutr Rev. 2003; 61:157–167. [PubMed: 12822704]
42. Crepaldi G, Maggi S. Sarcopenia and osteoporosis: a hazardous duet. J Endocrinol Invest. 2005; 28:66–68. [PubMed: 16550726]
43. Schoenfeld AJ, Nelson JH, Burks R, et al. Incidence and risk factors for lumbar degenerative disc disease in the United States military 1999–2008. Mil Med. 2011; 176:1320–1324. [PubMed: 22165663]
44. Bohatirchuk F. Aging and osteoarthritis. Can Med Assoc J. 1957; 76:106–114. [PubMed: 13383416]
45. Sinusas K. Osteoarthritis: diagnosis and treatment. Am Fam Physician. 2012; 85:49–56. [PubMed: 22230308]
46. Hsu JD, Furumasu J. Gait and posture changes in the Duchenne muscular dystrophy child. Clin Orthop Relat Res. 1993; 288:122–125. [PubMed: 8458124]
47. Madigan L, Vaccaro AR, Spector LR, et al. Management of symptomatic lumbar degenerative disk disease. J Am Acad Orthop Surg. 2009; 17:102–111. [PubMed: 19202123]
48. Lammers AR, German RZ, Lightfoot PS. The impact of muscular dystrophy on limb bone growth and scaling in mice. Acta anatomica. 1998; 162:199–208. [PubMed: 9831769]
49. Garris DR, Burkemper KM, Garris BL. Influences of diabetes (db/db), obese (ob/ob) and dystrophic (dy/dy) genotype mutations on hind limb bone maturation: a morphometric, radiological and cytochemical indices analysis. Diabetes Obes Metabol. 2007; 9:311–322.
50. Loeser RF. Age-related changes in the musculoskeletal system and the development of osteoarthritis. Clin Geriatr Med. 2010; 26:371–386. [PubMed: 20699160]
51. Adams MA, Roughley PJ. What is intervertebral disc degeneration, and what causes it? Spine (PhilaPa 1976). 2006; 31:2151–2161.
52. Johnell O, Kanis J. Epidemiology of osteoporotic fractures. Osteoporos Int. 2005; 16:S3–S7. [PubMed: 15365697]
53. Rossi DJ, Jamieson CH, Weissman IL. Stems cells and the pathways to aging and cancer. Cell. 2008; 132:681–696. [PubMed: 18295583]
54. Lavasani M, Robinson AR, Lu A, et al. Muscle-derived stem/progenitor cell dysfunction limits healthspan and lifespan in a murine progeria model. Nat Commun. 2012; 3:608. [PubMed: 22215083]

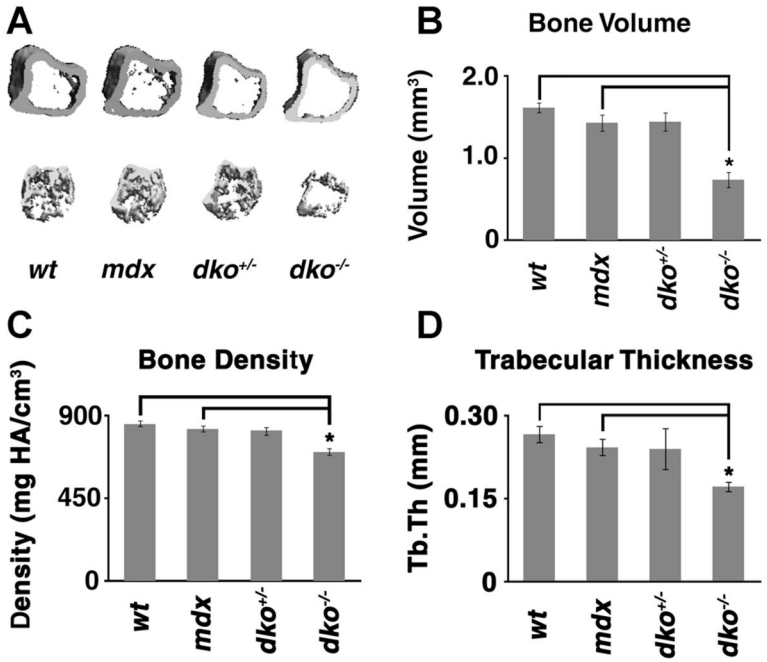

Figure 1.

Micro-CT analysis of the proximal tibia of $dko^{-/-}$ mice. Age-matched, 6 weeks old, male wild-type (*wt*), *mdx*, $dko^{+/-}$, and $dko^{-/-}$ mice were anesthetized and analyzed using micro-CT. The proximal tibia was selected for 3D evaluation. Representative images are displayed in (A). Proximal tibia bone volume (B), bone density (C), and trabecular thickness (Tb.Th; D) were determined. The mean values for each genotype are displayed and error bars represent one standard deviation above and below the mean. Asterisks (*) denote statistical differences with p values <0.005.

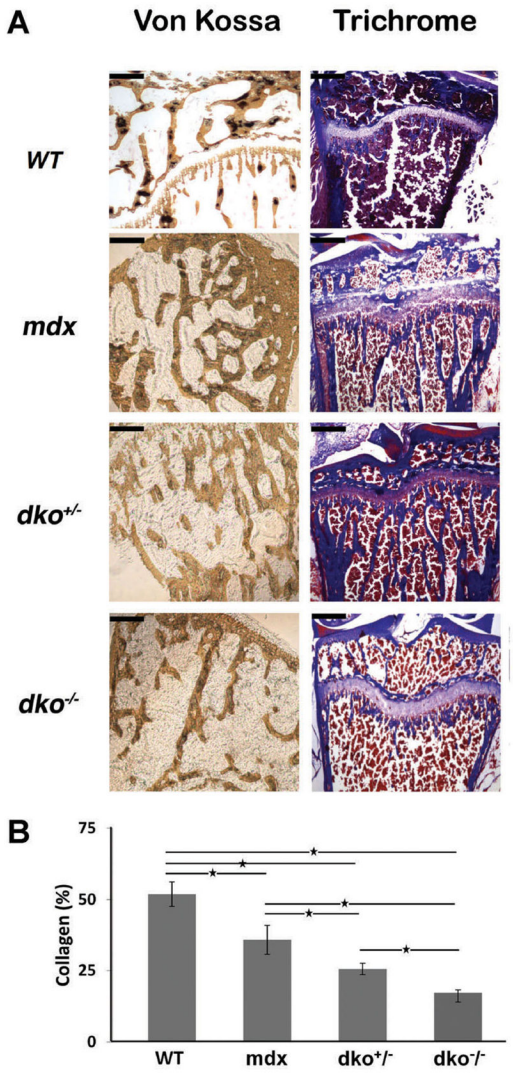

Figure 2.

Histological analysis of the proximal tibia from *dko*$^{-/-}$ mice. (A) Age-matched, 6 weeks old, male *wild-type*, *mdx*, *dko*$^{+/-}$, and *dko*$^{-/-}$ mice were sacrificed and the proximal tibia was processed for histological analysis with von Kossa and Masson trichrome staining. Representative images are shown. Scale bars in the upper left-hand corner represent 0.2 mm (at 4× magnification). (B) For trichrome analysis, the amount of collagen per area was determined for each genotype and the results are shown. The mean values for each genotype are displayed and error bars represent one standard deviation above and below the mean. Asterisks (*) denote statistical differences with p values < 0.05.

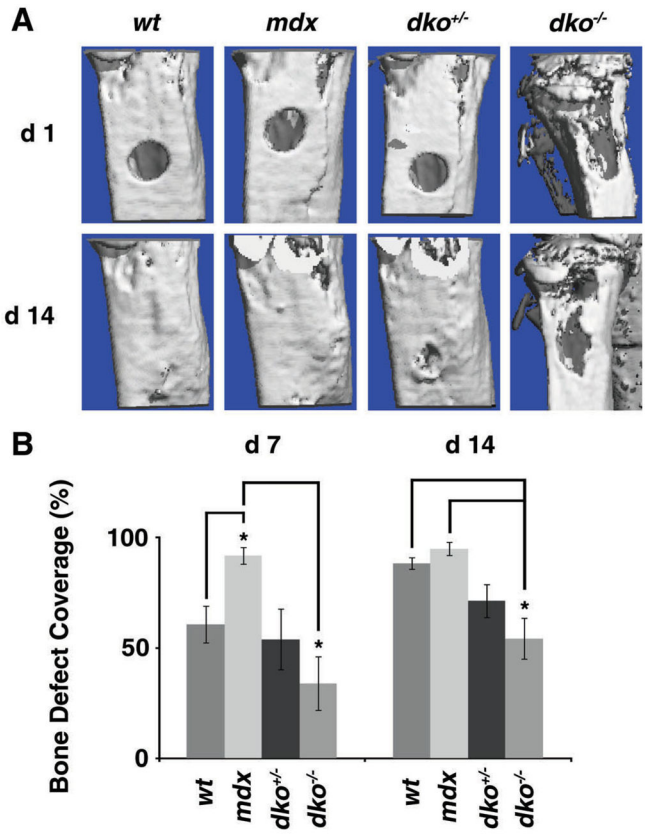

Figure 3.

Bone healing in $dko^{-/-}$ mice. (A) A spherical defect was created in the proximal tibia of age-matched, 5 weeks old, male wild-type (*wt*), *mdx*, $dko^{+/-}$, and $dko^{-/-}$ mice. The defects were analyzed by micro-CT 24 h after surgery and followed with serial micro-CT evaluations at post-operative day 7 (d7) and 14 (d14) to determine the amount of bone formation. Representative 3D images of the proximal tibia obtained via micro-CT analysis are displayed for POD1 (d1) and d14. (B) Amount of defect coverage was determined on d7 and d14 after surgery by comparing the size of the defect to the initial defect on d1. The mean values for each genotype are displayed and error bars represent one standard deviation above and below the mean. Asterisks (*) denote statistical differences with p values <0.05.

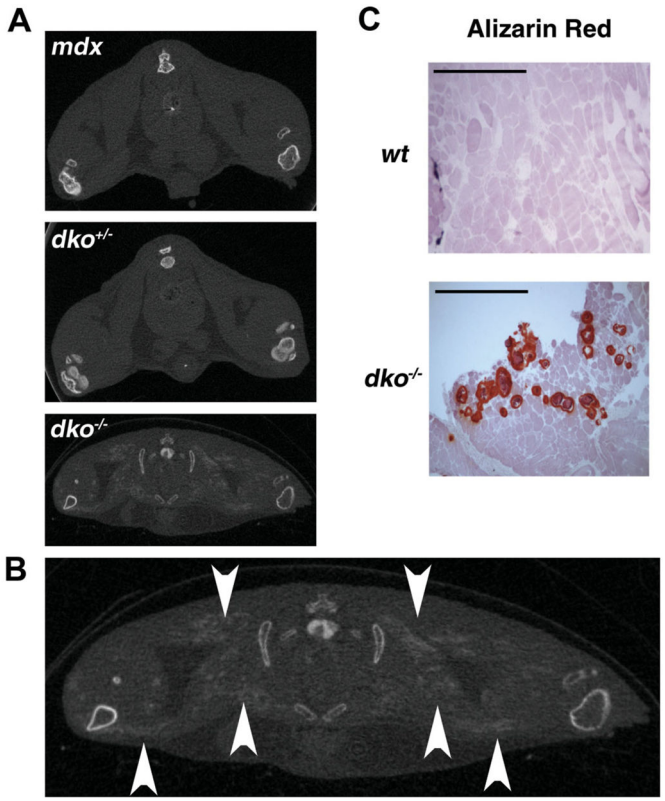

Figure 4.

Ectopic calcification in the soft tissues of *dko*$^{-/-}$ mice. (A) 7-week-old *mdx*, *dko*$^{+/-}$, and *dko*$^{-/-}$ mice were evaluated by micro-CT and representative images are shown to illustrate the presence of ectopic calcification (EC) in the proximal hind limb soft tissues of *dko*$^{-/-}$ mice exclusively. (B) A larger view of the micro-CT image from (A) with arrowheads demonstrating EC in a *dko*$^{-/-}$ mouse. (C) Skeletal muscle cryosections were prepared from the gluteus maximus of these mice and processed for histological analysis. Representative images obtained with alizarin red staining are shown. Scale bars in the upper left-hand corner represent 0.5 mm (at 4× magnification).

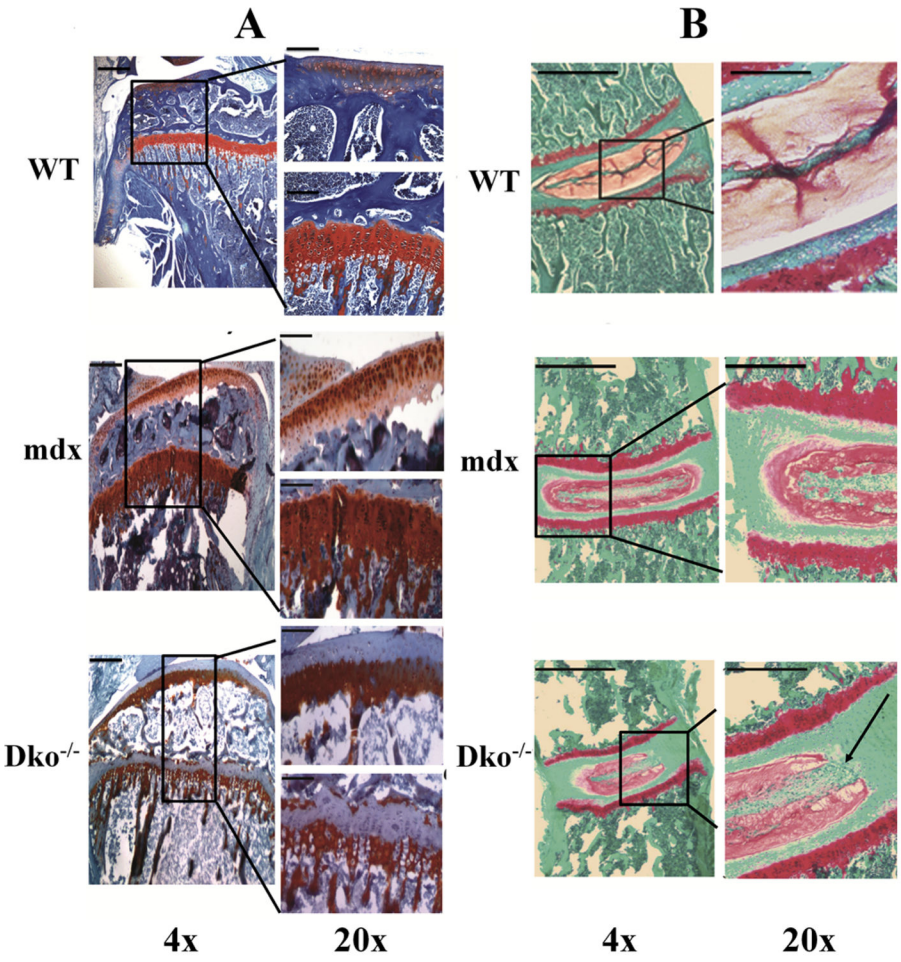

Figure 5.

Loss of proteoglycans from tibial articular cartilage and intervertebral discs of *dko*$^{-/-}$ mice. (A) Tibias and (B) spines were isolated from age-matched, male *wild-type*, *mdx*, *dko*$^{-/-}$ mice and processed for histology. Sections were stained with safranin O dye and counterstained with fast green. Representative images were taken at 4× and 20× magnification and demonstrate a loss of proteoglycans at the articular cartilage and growth plate surface in the *dko*$^{-/-}$ proximal tibia, and a loss of proteoglycans from the nucleus pulposus in the *dko*$^{-/-}$ intervertebral disc, as indicated by the arrow. Scale bars in the upper left-hand corner represent 0.2 mm (at 4×) and 0.1 mm (at 20× magnification) in (A), and 1 mm (at 4×) and 0.5 mm (at 20× magnification) in (B).